The Journal of Immunology

RESEARCH ARTICLE | OCTOBER 15 2002

IL-19 Induces Production of IL-6 and TNF-α and Results in Cell Apoptosis Through TNF-α[1] FREE

Yuan-Chun Liao; ... et. al

J Immunol (2002) 169 (8): 4288–4297.
https://doi.org/10.4049/jimmunol.169.8.4288

IL-19 Induces Production of IL-6 and TNF-α and Results in Cell Apoptosis Through TNF-α[1]

Yuan-Chun Liao,* Wei-Guang Liang,* Feng-Wei Chen,* Ju-Hui Hsu,† Jiann-Jou Yang,† and Ming-Shi Chang[2]*†

IL-10 is an immunosuppressive cytokine in the immune system. It was in clinical trail as an anti-inflammatory therapy for inflammatory bowel disease and various autoimmune diseases such as psoriasis, rheumatoid arthritis, and multiple sclerosis. IL-19 belongs to the IL-10 family, which includes IL-10, IL-19, IL-20, IL-22, melanoma differentiation-associated gene (MDA-7, IL-24), and AK155 (IL-26). Despite a partial homology in their amino acid sequences, they are dissimilar in their biologic functions. Little is known about the biologic function and gene regulation of IL-19. To understand the gene regulation of human IL-19, we identified a human IL-19 genomic clone and analyzed its promoter region. Five fusion genes containing different regions upstream of exon 1 linked to a luciferase reporter gene were expressed in the canine kidney epithelial-like Madin-Darby canine kidney cells. A fusion gene containing 394 bp showed luciferase activity 7- to 8-fold higher than the negative control of the promoterless fusion gene. We also isolated a full-length mouse cDNA clone. Mouse IL-19 shared 71% amino acid identity with human IL-19. Treatment of monocytes with mouse IL-19 induced the production of IL-6 and TNF-α. It also induced mouse monocyte apoptosis and the production of reactive oxygen species. Taken together, our results indicate that mouse IL-19 may play some important roles in inflammatory responses because it up-regulates IL-6 and TNF-α and induces apoptosis. ***The Journal of Immunology*****, 2002, 169: 4288–4297.**

The inflammatory response is a key component of host defense, but excessive inflammation, such as occurs in arthritis or septic shock, can be harmful or even fatal (1). IL-10 was originally described as a cytokine synthesis-inhibitory factor due to its inhibitory effect on cytokine production (2). Because IL-10 suppresses the release and function of a number of proinflammatory cytokines such as IL-1, TNF-α, and IL-6, it is a normal endogenous feedback factor for the control of immune responses and inflammation (2, 3). Autoimmune models of rheumatoid arthritis, thyroiditis, and collagen-induced arthritis and a model of herpetic stromal keratitis all suggest negative regulatory roles of IL-10 in limiting inflammation and immunopathology (3). However, IL-10 is also a stimulatory factor for mast cells, B cells, and thymocytes (4–6), and has been shown to be pleiotropic and to act on many other cell types, including monocytes/macrophages, T cells, NK cells, neutrophils, endothelial cells, and PBMC (7, 8).

Several new members of the IL-10 family, including IL-19, IL-20, IL-22, melanoma differentiation-associated gene (MDA)[3]-7 (IL-24), and AK155 (IL-26), have only recently been discovered. The IL-19, IL-20, and MDA-7 (IL-24) genes have been mapped on chromosome 1q31–32, a region where IL-10 is located. The two other IL-10-related cytokines, AK155 (IL-26) and IL-22, are on chromosome 12q15 (9). Overexpression of IL-20 in transgenic mice causes neonatal death as well as skin abnormalities, including aberrant epidermal differentiation (10). IL-22 was originally identified as a gene induced by IL-9 in murine T lymphocytes. Stimulation of HepG2 human hepatoma cells with IL-22 up-regulated the production of acute phase reactants like serum amyloid A, α_1-antichymotrypsin, and haptoglobin (11, 12). Expression of MDA-7 was up-regulated in wound healing and during the in vitro differentiation of a melanoma cell line (13, 14). AK155 is induced by transformation of T lymphocytes with *Herpesvirus saimiri*, but its biologic activities and receptor remain poorly understood (9, 15). Little is known about the biologic function of IL-19, except that it is expressed by LPS- or GM-CSF-activated monocytes (16). Our aims, therefore, were to understand the gene regulation of human IL-19 and the biologic function of IL-19. For these aims, we isolated the human genomic clone and determined its promoter sequence. We also isolated the mouse IL-19 cDNA and identified the biologic functions of the IL-19 recombinant protein.

Materials and Methods

Identification of human genomic IL-19

A homology screening of the National Center for Biotechnology Information human high throughput genome database (http://www.ncbi.nlm.nih.gov) using the human IL-19 cDNA sequences as a query was conducted using a basic Blast search. The human genomic clone (clone identification, RP11-237C22) was identified (accession number AF276915) and purchased from Research Genetics (Huntsville, AL). The genomic DNA was isolated from the BAC clone and used in the PCR amplification of the promoter fragments.

Isolation of full-length human cDNA clone

The full-length human cDNA clone[4] was obtained by repetitive 5′ RACE using anchor primers and the gene-specific antisense primers: 5′-gatatagct

*Graduate Institute of Biochemistry, Medical College, National Cheng Kung University, Tainan, Taiwan; and †Chi-Mei Medical Center, Tainan, Taiwan

Received for publication March 14, 2002. Accepted for publication August 20, 2002.

The costs of publication of this article were defrayed in part by the payment of page charges. This article must therefore be hereby marked *advertisement* in accordance with 18 U.S.C. Section 1734 solely to indicate this fact.

[1] This work was supported by Grant NSC 89-2323-B006-004 from the National Science Council, Taiwan, Republic of China.

[2] Address correspondence and reprint requests to Dr. Ming-Shi Chang, Graduate Institute of Biochemistry, National Cheng Kung University, College of Medicine, Tainan, Taiwan 70. E-mail address: mschang@mail.ncku.edu.tw

[3] Abbreviations used in this paper: MDA, melanoma differentiation-associated gene; MDCK, Madin-Darby canine kidney; ROS, reactive oxygen species; SNP, single-nucleotide polymorphism; β-gal, β-galactosidase; CL, chemiluminescence; PI, propidium iodide.

[4] The nucleotide sequences reported in this paper have been submitted to GenBank database. Human IL-19 promoter sequence, AF454433; human IL-19 cDNA, AF453946; mouse IL-19 cDNA, AF453945.

0022-1767/02/$02.00

gattaatca-3′ (reverse transcription primer); 5′-taaactccccatctccatgcaa-3′ (first PCR); 5′-caattctatgtccatgcagaaaaat-3′ (second PCR). After three rounds of 5′ RACE, the 5′ end of exon 1 were determined.

Construction of promoter-luciferase fusion gene

Five different regions upstream of exon 1 of the human IL-19 gene were amplified by PCR from the DNA of the BAC clone RP11-237C22. Five fragments (pA, pB, pC, pD, pE) containing different lengths of sequences upstream of exon 1 and 247 bp (1 to 247) of exon 1 were ligated into the vector of the promoterless luciferase gene (pGL3 enhancer). pA contains 2105 bp (from −1858 to 247). pB contains 1365 bp (from −1118 to 247). pC contains 1085 bp (from −838 to 247). pD contains 713 bp (from −466 to 247). pE contains 394 bp (from −147 to 247). We generated five fusion genes by cloning these fragments into the *Sac*I-*Xho*I site of the pGL3 enhancer plasmid vector containing the entire coding sequences of firefly luciferase and SV40 enhancer (Promega, Madison, WI).

Transfection and luciferase activity assay

The fusion gene was used along with the promoterless pGL3 enhancer plasmid DNA in the transfection of the canine kidney epithelial-like Madin-Darby canine kidney (MDCK)[4] cells. Cells at a density of 3×10^5/well in a six-well plate were transfected with 1 μg of plasmid DNA from the fusion gene and 0.4 μg of the β-galactosidase (β-gal) gene which was used as an internal transfection efficiency control by using 1 μl of LipofectAMINE 2000 reagent (Invitrogen, Carlsbad, CA). Twenty-four hours after transfection, the medium was replaced with fresh medium. Forty-eight hours after transfection, the cells were collected, and the luciferase activity was analyzed according to the protocol of the luciferase assay system (Promega). To obtain internal control of β-gal gene transfection, the cell lysate was also used for β-gal activity analysis. The luciferase activity from each promoter-fusion gene was divided by β-gal activity to obtain the true representation of luciferase activity from each promoter-luciferase fusion gene.

Isolation of mouse IL-19 cDNA

A partial murine cDNA clone was isolated by PCR amplification from mouse embryo cDNA (Clontech, Palo Alto, CA). A pair of primers (sense primer, 5′-agagccatccaagctaaggacacctt-3′; and antisense primer, 5′-gcat tggtggcttcctgcctgcagt-3′) designed from human cDNA sequences was used in PCR amplication. The full-length cDNA clone was further obtained by 5′ and 3′ RACE.

Protein expression and purification

A cDNA clone coding for the human and mouse IL-19 sequences from leucine to histidine (aa 25–176) was inserted into pET32 EK/LIC (Novagen, Madison, WI). The protein was found mostly in the inclusion bodies and was purified to >95% by a series of affinity chromatography and refolding. Before in vitro use, all preparations of IL-19 recombinant protein were found to contain <2 ng/ml LPS endotoxin by the detection methods of *Limulus* amebocyte lysate. The human IL-19 was also expressed in the yeast vector of *Pichia pastoris*, and the protein was purified by a series of affinity chromatography.

Isolation of mouse monocytes

Mouse monocytes were prepared from the spleen of 8- to 10-wk-old male mice. Spleen cells were depleted of erythrocytes. Monocytes were allowed to adhere for 30 min at 37°C and 5% CO_2. The nonadherent cells were then removed by three washes with warm medium. The monocytes were >95% pure, as determined by Liu's staining and contained >98% viable cells.

In vitro biological function analysis

The monocytes were cultured at a concentration of 5×10^6 cells/ml in a six-well plate and then treated with different concentrations of mouse IL-19 protein for 8 h. After incubation, the monocyte supernatants were collected, and the production of IL-6 and TNF-α was measured by ELISA kits (R&D, Minneapolis, MN). To analyze induction of IL-6 and TNF-α transcript by IL-19, the monocytes were treated with mouse IL-19 (100 ng/ml) or LPS (50 ng/ml) for 4 h. Total RNA was isolated from the monocytes. RT-PCR was performed with IL-6- or TNF-α-specific primers using total RNA as templates. Amplified PCR fragments were run on gel electrophoresis. Specific primers for β-actin were also used to amplify a PCR fragment and run on gel as an internal control. IL-6-specific primers used are 5′- tgt gca atg gca att ctg at-3′ (sense) and 5′-gga aat tgg ggt agg aag ga-3′ (antisense). TNF-α-specific primers used are 5′-ccc caa agg gat gag aag tt-3′ (sense) and 5′-gtg ggt gag gag cac gta gt-3′ (antisense).

Mouse β-actin-specific primers used are 5′-ggg aat ggg tca gaa gga ct-3′(sense) and 5′-ttt gat gtc acg cac gat tt-3′(antisense).

To analyze interaction of IL-19 and IL-10, monocytes were pretreated with IL-10 (50 ng/ml) or IL-19 (50 ng/ml) for 2 h, and then the other cytokine, either IL-19 or IL-10, was added to the culture. Six hours after coincubation with both cytokines, monocyte supernatants were collected together with the controls (PBS or single cytokine treatment). Production of IL-6 and TNF-α from these monocytes was analyzed.

In the experiment to test the effect of cycloheximide, 1 h after IL-19 (100 ng/ml) had been added to the culture, cycloheximide was added at a concentration of 0.3 mM and incubated with cells for another 7 h.

Cell viability analysis

Cell viability was analyzed by propidium iodide (PI) staining and annexin V assay (Clontech). Mouse monocytes were treated with PBS or mouse IL-19 (100 ng/ml) alone or combined with TNF-α Ab for 12 h. After treatment, cells were stained with PI and then analyzed by flow cytometry (FACScan; BD Biosciences, San Juan, CA). For the annexin V assay, cells were treated as above, harvested, and then resuspended in 1× binding buffer at a concentration of 1×10^6 cells/ml. Annexin V-FITC (5 μl) was added to 100 μl of the cell solution. The cells were gently vortexed, incubated in the dark for 15 min at room temperature, and then analyzed by flow cytometry (FACScan).

DNA fragmentation by gel electrophoresis

Using the method described by Oren and Prives (17), mouse lymphocytes (5×10^6 cells/well) were treated with mouse IL-19 for 12 h. After treatment, the culture medium was removed, and the cells were washed twice with PBS and harvested. Then the cells were fixed with 1 ml 70% ethanol. After storage overnight at 4°C, the ethanol was removed, and the cells were resuspended in 1 ml phosphate-citric acid buffer with 0.2 M Na_2HPO_4 and 0.1 M citric acid (pH 7.8) and maintained in this solution at room temperature for 60 min with occasional shaking. This treatment extracts low molecular mass DNA from apoptotic cells but has no effect on the DNA content of nonapoptotic cells (18). The cell suspension was centrifuged at 2000 rpm for 5 min. The supernatant containing low molecular mass DNA was collected for analysis of internucleosomal DNA degradation by agarose gel electrophoresis.

Measurement of reactive oxygen species (ROS) produced from monocytes

To evaluate the effect of mouse IL-19 on ROS production by monocytes in vitro, mouse monocytes (1×10^6 cells) were incubated at 37°C with different concentrations of mouse IL-19 (0–50 ng/ml) for various times. The ROS activities were determined at the end of the incubation.

Monocytes were collected and resuspended in 0.2 ml PBS. The chemiluminescence (CL) count was measured in a completely dark chamber of the Chemiluminescence Analyzing System. After a 100-s background level determination, 0.5 ml of 25 mM luminol in PBS (pH 7.4) was injected into the sample. The CL was monitored continuously for an additional 600 s. To analyze the effect of TNF-α Ab on ROS production, the Ab was added to monocytes 30 min before or after the addition of IL-19 (100 ng/ml), or else both reagents were added at the same time. After incubation with both reagents for another 30 min, ROS production from monocytes was measured by CL count.

Results

Genomic structure of the human IL-19 gene

Human IL-19 genomic clone (clone identification, RP11-237C22) was identified by homology search against a human high throughput genome database. The 5′ end of untranslated sequences of the human cDNA was obtained by a series of repeated 5′ RACE. After obtaining the full-length cDNA clone, the cDNA sequence was compared with the human genomic sequences to locate the exon/intron boundaries. The 5′ untranslated sequence and the potential promoter sequence is shown in Fig. 1. The locations of the introns in this region are indicated by the two arrows at nt 250 and nt 937

There are two additional exons and two introns in the 5′ untranslated region (Fig. 2). Therefore, human IL-19 gene contains seven exons and six introns. As Fig. 2 shows, the exon/intron junctions conform to the GT/AT rule. The human IL-19 protein is encoded by exon 3 to exon 7.

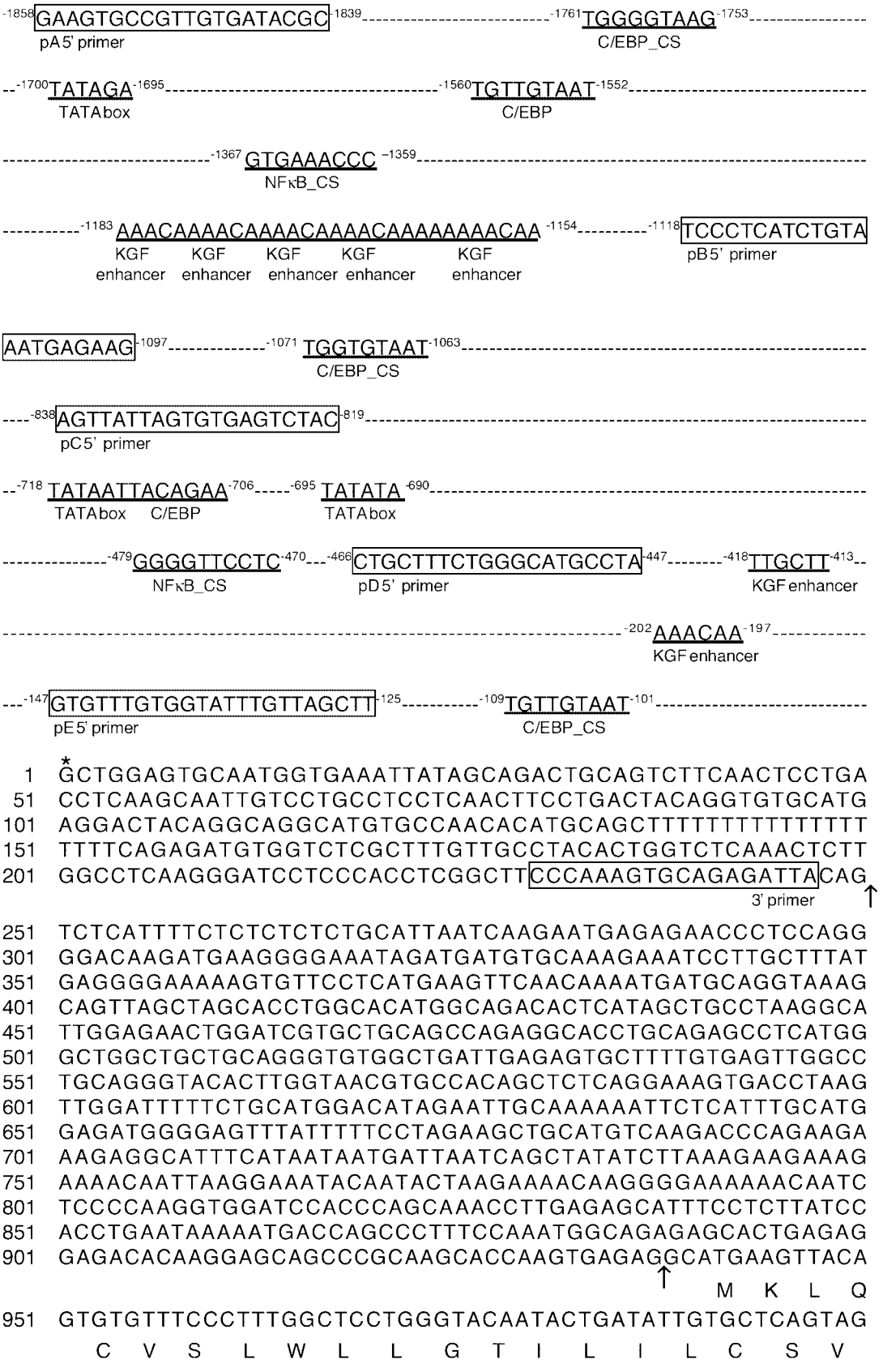

FIGURE 1. The 5′-untranslated region of human IL-19 cDNA and the promoter sequences. The exon/intron junctions in the 5′ untranslated region are indicated by the two arrows. The potential transcription start site is designated as number 1 and shown by an asterisk over the nucleotide. The potential transcription factor-binding sites are underlined. The five 5′ sense primers and one 3′ antisense primer used in the construction of five fragments (pA, pB, pC, pD, and pE) for promoter analysis are enclosed in boxes.

Exon 1	Intron 1	Exon 2
AGA TTA CAG	gtgtgagcc… (4593 bp) …. tctttccag	TCT CAT TTT
Exon 2	**Intron 2**	**Exon 3**
AAG TGA GAG	gtgaagctc… (2259 bp) …. tttctgcag	GC ATG AAG M K
Exon 3	**Intron 3**	**Exon 4**
AGA GCC ATC R A I	gtgagtatg… (151 bp) …. cctccacag	CAA GCT AAG Q A K
Exon 4	**Intron 4**	**Exon 5**
ATC ATT AAG I I K	gtattggcc… (2613 bp) …. tgtttgtag	CCC CTA GAT P L D
Exon 5	**Intron 5**	**Exon 6**
CGG CAA TGT R Q C	gtgagtcac… (1002 bp) …. ttatcacag	CAG GAA CAG Q E Q
Exon 6	**Intron 6**	**Exon 7**
TAT GAT CAG Y D Q	gtaagatct… (1449 bp) …. tgatttcag	CTG GAG GTC L E V

FIGURE 2. Sequences of the exon/intron junctions of the human IL-19 gene. Exon sequences are shown in uppercase letters; intron sequences are shown in lowercase letters. The encoded amino acids are indicated below the exon sequences.

During the process of isolating the 5′ untranslated region, we also found another alternatively spliced variant in which the first exon ends at nt 91 and the second exon begins at nt 251. This transcript variant therefore has a longer intron, 4752 bp instead of 4593 bp.

Promoter activity of human IL-19

To characterize the DNA sequences involved in the human IL-19 gene expression, we used PCR to amplify five potential promoter fragments (A, B, C, D, and E) by using a human genomic clone as a template. The sizes of the PCR fragments ranged from 2.1 kb to 400 bp upstream of exon 1 (Figs. 1 and 3*A*). These potential promoter regions were subcloned into the pGL3 enhancer vector containing the luciferase gene along with the SV40 enhancer to generate five fusion genes: *pA*, *pB*, *pC*, *pD*, and *pE*. During our isolation of the full-length cDNA clone, we isolated partial cDNA sequences from human kidney RNA. We also performed Northern blots to analyze tissue distribution of IL-19 and found that the 1.35-kb transcript of IL-19 was expressed in heart, brain, liver, and kidney. In these four tissues, kidney and heart expressed higher amount than brain and liver. Therefore, we used the MDCK cells and human embryonic kidney 293 cells for the analysis of promoter activity. After transfection of the MDCK cells with the fusion gene, the luciferase activities were analyzed. All five promoter fragments contained at least one or several TATA boxes. All showed some promoter activity, with the *pE* fusion gene the highest, 7- to 8-fold higher than the negative control of the promoterless pGL3 enhancer vector (Fig. 3*B*). This experiment was repeated five times with similar results. The luciferase activity in 293 cells was similar to that of MDCK cells. The promoter region[4] 2.1 kb contained several transcription factor-binding sites: several copies of keratinocyte-enhancer; TATA box; NF-κB; AP-1; AP-2; E1A-CS; GATA-1; SP-1; P53; and C/EBP (Fig. 1). Previous study

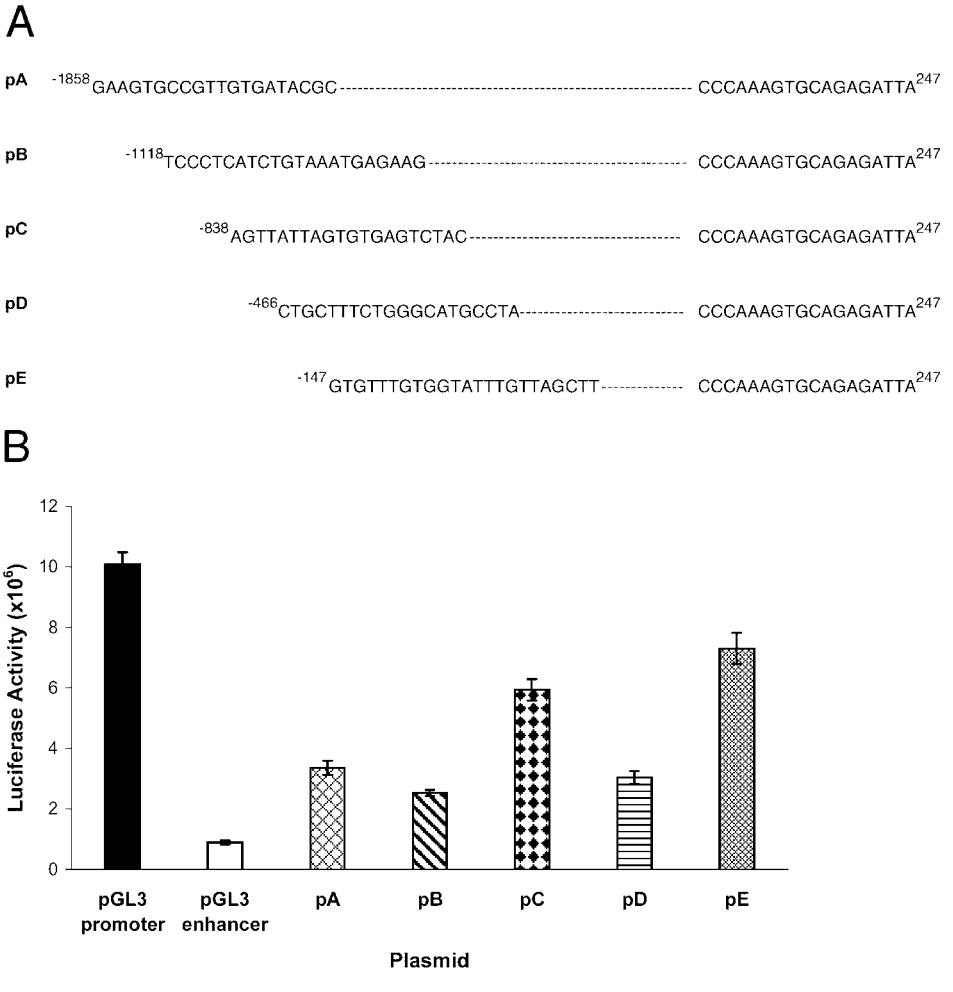

FIGURE 3. Effect of the human IL-19 promoter on luciferase activity. Potential transcription start site was designated as nucleotide 1. *A*, Five fragments (pA, pB, pC, pD, pE) containing different lengths of sequences upstream of exon 1 and 247 bp of exon 1 were ligated into the vector of the promoterless luciferase gene (pGL3 enhancer). pA contains 2105 bp (from −1858 to 247). pB contains 1365 bp (from −1118 to 247). pC contains 1085 bp (from −838 to 247). pD contains 713 bp (from −466 to 247). pE contains 394 bp (from −147 to 247). *B*, These five fusion genes were transfected into the MDCK cells, along with the negative control promoterless vector (pGL3 enhancer) and the positive control vector (pGL3 promoter). The luciferase activity data presented here are averages of triplicate samples.

has shown that IL-19 is inducible by LPS (16). We added LPS into the transfectants and found that luciferase activity was not inducible by LPS. This could be due to the constitutive expression of IL-19 in kidney cells.

Isolation and characterization of mouse IL-19 cDNA

The full-length mouse cDNA clone[4] (~1 kb long) was isolated by 5′ and 3′ RACE. The 3′-untranslated region contained only one ATTTA mRNA-destabilizing segment. Hydropathic analysis predicts a hydrophobic signal peptide of 24 aa. Beginning with leucine (residue 25), the mature protein, which contains 152 aa, has a predicted molecular mass of 17 kDa. Three potential *N*-linked glycosylation sites were detected in the amino acid sequences, only two of which, NVT and NAT, are identical with those in human IL-19. The third, NCS, is not present in human IL-19. The protein contains six cysteines the positions of which are identical with those in human IL-19 (Fig. 4). The amino acid sequences of mouse IL-19 showed 75% similarity and 71% identity with those in human IL-19, and the genomic structure of mouse IL-19 is similar to that of human IL-19. Locations of exon/intron boundaries in the mouse gene are also indicated in Fig. 4.

Expression and purification of IL-19 recombinant protein

To express the recombinant IL-19 in *Escherichia coli*, we constructed an expression vector that contained a coding region from leucine (residue 25) to histidine (residue 170) downstream of the fusion protein sequence (thioredoxin). The predicted molecular mass of mouse IL-19 containing fusion protein (thioredoxin) is ~35 kDa. Treatment of mouse IL-19 fusion protein with enterokinase to cleave off thioredoxin resulted in the disappearance of the 35-kDa band and the formation of a single 17-kDa band on the SDS-PAGE after protein was purified and reduced with 2-ME (data not shown). Recombinant human IL-19 was similarly expressed and showed the same purification pattern as mouse IL-19. Both mouse and human recombinant protein after a series of chromatography was found to contain <2 ng/ml LPS endotoxin. Human IL-19 was also expressed in the yeast *P. pastoris.* The recombinant protein produced from *P. pastoris* showed three bands on SDS-PAGE after affinity chromatography purification. Amino acid determination of the three bands by mass spectrophotometry showed that all three proteins were human IL-19 (data not shown).

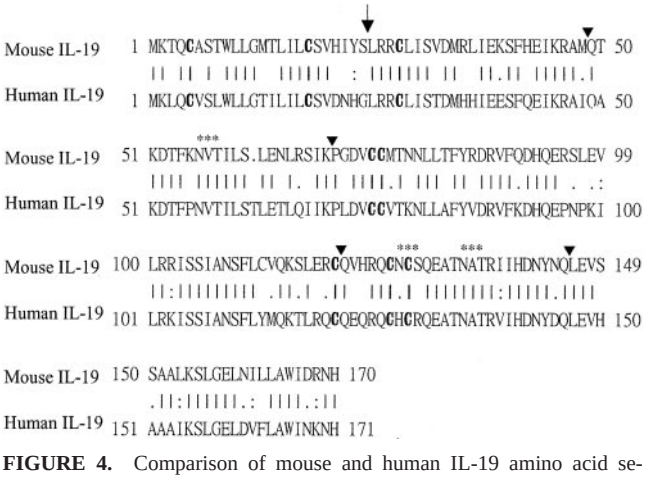

FIGURE 4. Comparison of mouse and human IL-19 amino acid sequences. Identical amino acid sequences are indicated by vertical line. Similar amino acid sequences are indicated by .:. The six conserved cysteines are in bold type. ***, Potential *N*-linked glycosylation sites. Signal peptide cleavage sites is indicated by ↓. ▼, Location of mouse IL-19 introns.

Mouse IL-19 stimulated monocytes to produce IL-6 and TNF-α

To determine the effects of mouse IL-19 on the production of cytokines by monocytes, the monocytes were incubated with various concentrations of mouse IL-19 for 8 h, after which the level of cytokine production in the supernatant of monocytes was determined by ELISA. As shown in Fig. 5, monocytes incubated in PBS alone at 37°C did not produce IL-6 and TNF-α. However, the amount of IL-6 (Fig. 5*A*) and TNF-α (Fig. 5*B*) produced by monocytes increased with the addition of mouse IL-19. The increase of these two cytokines was dosage dependent on IL-19.

LPS endotoxin can also induce monocytes to produce IL-6 and TNF-α production. To prove that the production of IL-6 and TNF-α from IL-19 treatment was not due to the contamination of LPS endotoxin in the recombinant protein, the protein was heat-denatured at 100°C for 10 min, a condition under which LPS endotoxin cannot be denatured. The heat-denatured protein was added to monocytes to test its biologic activity. The result showed that the heat-denatured protein had lost its activity (Fig. 5). Therefore, the activities we observed were not due to contamination of the LPS endotoxin. Human IL-19 was shown to have the same activities on human monocytes as mouse IL-19 has on mouse monocytes (data not shown).

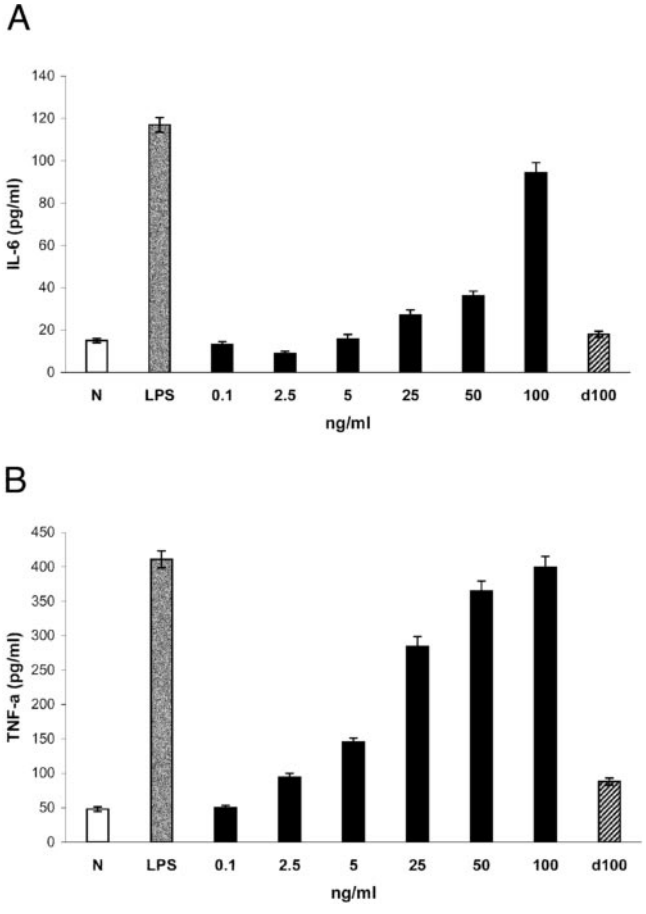

FIGURE 5. Production of mouse IL-6 and TNF-α by mouse monocytes in response to increasing concentration of mouse IL-19. *A*, Mouse monocytes (5×10^6 cells/ml) were cultured in a six-well plate with increasing concentrations of mouse IL-19 for 8 h, and the production of mouse IL-6 was determined by ELISA. *B*, Mouse monocytes (5×10^6 cells/ml) were cultured in a six-well plate with increasing concentrations of mouse IL-19 for 8 h, and the production of mouse TNF-α was determined by ELISA. The control sample was incubated with PBS only. Denatured mouse IL-19 was heat denatured at 100°C for 10 min. Endotoxin LPS used as a positive control was added at a concentration of 100 ng/ml.

Mouse IL-10 has been shown to be inactive on human monocytes. In contrast, we found that mouse IL-19 protein is active on human monocytes but that human IL-19 is inactive on mouse monocytes (data not shown). This result also provided the evidence that the activity observed from IL-19 treatment is not due to LPS endotoxin.

To investigate whether induction of IL-6 and TNF-α was regulated at the transcriptional level, total RNA was isolated from IL-19- or LPS-treated monocytes. The levels of IL-6 and TNF-α transcripts were analyzed by RT-PCR. As shown in Fig. 6, both IL-6 and TNF-α transcripts were induced in monocytes stimulated with IL-19. Induction of IL-6 and TNF-α transcripts may not require de novo protein synthesis because the addition of cycloheximide did not inhibit the induction (data not shown).

Previous study has shown that IL-10 inhibited IL-6 and TNF-α production in monocytes. Therefore, interaction between IL-10 and IL-19 was analyzed by treating monocytes with both cytokines at different times. As shown in Fig. 7, pretreatment of monocytes with IL-10 for 2 h followed by IL-19 abolished both IL-6 and TNF-α production by IL-19 (Fig. 7, *A* and *B*, column C). However, treatment of monocytes with IL-19 followed by IL-10 blocked only part of IL-19 activity on IL-6 induction, whereas a majority of TNF-α production was inhibited (Fig. 7, *A* and *B*, Column D). This result demonstrated that interactions between IL-19 and IL-10 in the regulation of IL-6 and TNF-α may be different.

Both LPS and IL-19 induced IL-6 and TNF-α. Therefore, we also added LPS and IL-19 together to the monocytes and analyze whether both have any synergistic effect. The result demonstrated there was no synergistic effect (data not shown).

IL-19-induced monocyte apoptosis

During the incubation of monocytes with IL-19, trypan blue staining showed a decrease in cell viability. We therefore further analyzed cell apoptosis using three methods. Mouse monocytes were treated with IL-19 for 12 h, and then cell viability was measured by PI staining, annexin V staining, and DNA fragmentation. As shown in Fig. 8*A*, monocytes treated with 100 ng/ml IL-19 resulted in 33% cell death (Fig. 8*Ac*), whereas the control showed only 13–16% cell death (Fig. 8*A*, *a* and *b*). LPS endotoxin produced 23% cell death (Fig. 8*Ad*). In contrast, heat-denatured IL-19 also showed only 17% cell death (Fig. 8*Ae*). Early in apoptosis, the phosphatidylserine in the inner membrane translocates to the outer surface of the plasma membrane and has a high affinity for annexin V, which makes annexin V staining an alternative method to demonstrate cell apoptosis. Fig. 8*B* shows that treatment of monocytes with mouse IL-19 increased the population of annexin V-stained dead cells (Fig. 8*Bb*). LPS endotoxin also induced cell death (Fig. 8*Bc*). This apoptotic effect of IL-19 may be due to the production of TNF-α, because addition of both IL-19 and TNF-αAb abolished the apoptotic effect of IL-19. To further verify the apoptotic effect of IL-19, after IL-19 treatment, DNA fragmentation analysis was performed. The results showed that mouse IL-19 induced DNA fragmentation of monocytes and that the extent of DNA fragmentation was dosage dependent on IL-19 (*lanes 3-7*) in Fig. 8*C*.

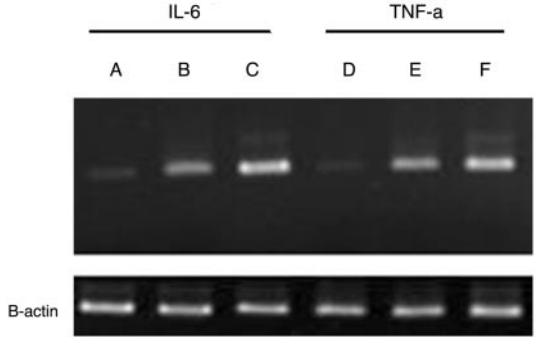

FIGURE 6. Mouse IL-19 induced IL-6 and TNF-α transcripts in monocytes. The monocytes were treated with mouse IL-19 (100 ng/ml) or LPS (50 ng/ml) for 4 h. Total RNA was isolated from the monocytes. RT-PCR was performed with IL-6- or TNF-α-specific primers using total RNA as templates. Amplified PCR fragments were run on gel electrophoresis. *Lanes A–C* are PCR fragments of IL-6; *lanes D, E,* and *F* are PCR fragments of TNF-α. Monocytes were treated with PBS (*lanes A* and *D*); *lanes B* and *E,* IL-19; *lanes C* and *F,* LPS. PCR fragment of β-actin was amplified as an internal control and shown under each lane.

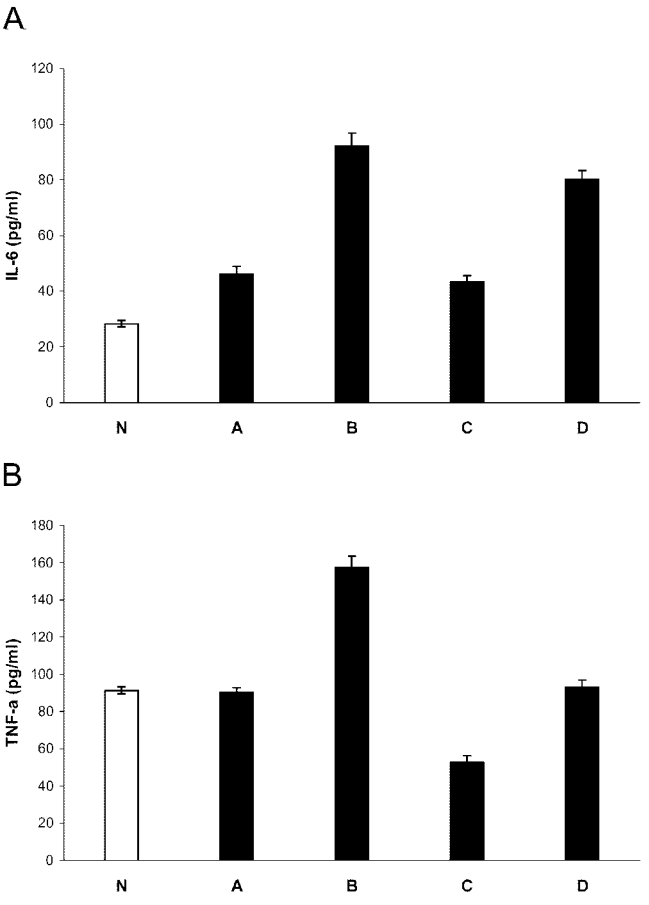

FIGURE 7. Interaction of IL-19 and IL-10 on IL-6 and TNF-α production. The mouse monocytes were incubated with IL-19 alone, IL-10 alone, or both cytokines added at different times (2 h apart). Eight hours after incubation, monocyte supernatants were collected and cytokines produced were measured by ELISA. *A,* Production of IL-6; *B,* production of TNF-α. Column N, PBS; column A, IL-10 alone; column B, IL-19 alone; column C, IL-10 for 2 h followed by IL-19; column D, IL-19 for 2 h followed by IL-10.

Mouse IL-19 induced monocytes to produce ROS

Exposure to certain cytokines induces marked transient increases in the intracellular level of ROS. For example, exposure to TNF-α or IL-1β increases intracellular levels of ROS in NIH3T3 fibroblasts, which suggests that ROS may act as signaling intermediates for TNF-α and IL-1β. These highly reactive ROS molecules regulate many important cellular events in response to TNF-α, including transcription factor activation (NF-κB), cellular proliferation, and apoptosis. Mouse IL-19 induced TNF-α production and resulted in cell apoptosis. To test whether this effect was mediated through the production of ROS, we treated mouse monocytes with

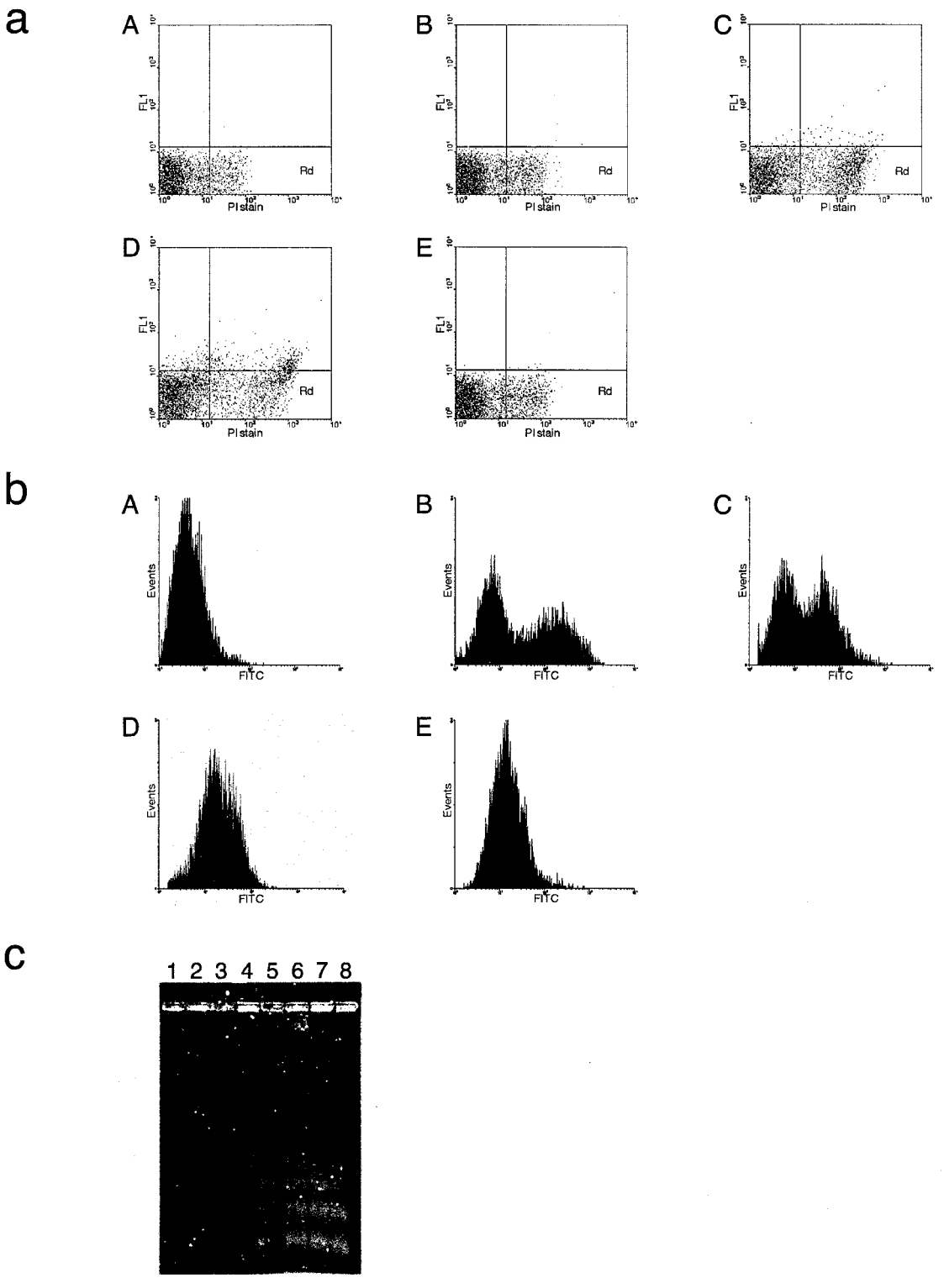

FIGURE 8. mIL-19 induced cell apoptosis in mouse monocytes revealed by PI staining (*A*), annexin V staining (*B*), and DNA fragmentation (*C*). *A*, The monocytes were treated with murine IL-19 for 12 h and washed twice with PBS after incubation. Then the cells were stained with 1 ml of solution containing 100 μg/ml PI at room temperature for 15 min. The rectangle marked Rd in the lower right quadrant of *a–e* indicates the region of dead cells. It is presented by percentage of dead cells. *a*, murine IL-19, 0 ng/ml, Rd, 13.33%; *b*, PBS, Rd, 15.98%; *c*, mIL-19, 100 ng/ml, Rd, 33.1%; *d*, LPS = 100 ng/ml, Rd, 23.16%; *e*, denatured mIL-19, 100 ng/ml, Rd, 17.26%. *B*, Mouse monocytes were treated with mIL-19 or LPS or TNF-α Ab as follows: *a*, PBS; *b*, mIL-19 = 100 ng/ml; *c*, LPS = 100 ng/ml; *d*, mIL-19 = 100 ng/ml and TNF-α Ab; *e*, TNF-α Ab alone. The apoptotic cells were stained by annexin V after 12 h treatment and then analyzed by flow cytometry. *C*, Mouse monocytes were treated with different concentrations of mIL-19 as follows: *lane 1*, mIL-19 = 0 ng/ml; *lane 2*, PBS; *lane 3*, mIL-19 = 2.5 ng/ml; *lane 4*: mIL-19 = 5 ng/ml, *lane 5*, mIL-19 = 25 ng/ml; *lane 6*, mIL-19 = 50 ng/ml; *lane 7*, mIL-19 = 100 ng/ml; *lane 8*, LPS = 100 ng/ml. The gel was visualized by staining with ethidium bromide.

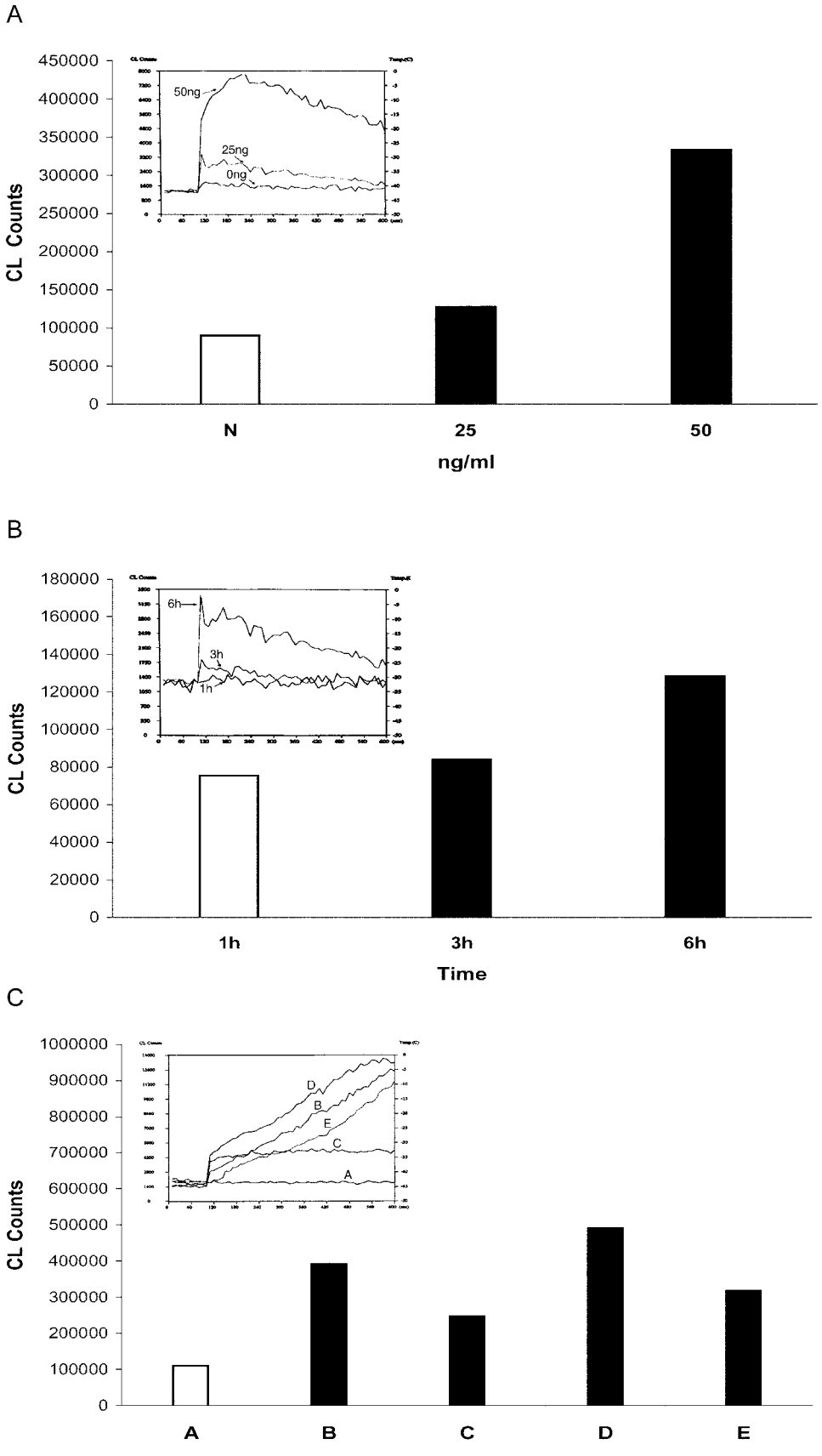

FIGURE 9. Effects of mIL-19 on ROS production in mouse monocytes measured by CL detector. *A*, Mouse monocytes treated with different concentrations of mIL-19 for 6 h, and ROS generation were measured by CL detector; *B*, mouse monocytes treated with the same concentration of mIL-19 (25 ng/ml), and the luminescence of ROS was measured at 1, 3, and 6 h of incubation. *C*, Effect of TNF-α Ab on inhibition of ROS production in mouse monocytes. Mouse monocytes were treated with IL-19 alone or incubated with both IL-19 and TNF-αAb, but each was added at different times. Monocytes were incubated with both reagents for another 30 min, and ROS production was measured. Column A, PBS; column B, IL-19 alone; column C, TNF-α Ab for 30 min followed by IL-19; column D, IL-19 for 30 min followed by TNF-α Ab; column E, both IL-19 and TNF-α Ab were added together. Final concentration of IL-19 was 100 ng/ml, and that of TNF-α Ab was 0.2 μg/ml.

various concentrations of IL-19 for various lengths of time. Monocytes treated with IL-19 for 6 h showed an increase in ROS formation in a dose-dependent manner (Fig. 9*A*). When monocytes were treated with IL-19 at the concentration of 25 ng/ml, ROS production increased with time (Fig. 9*B*). However, production of ROS decreased rapidly after 12 h incubation (data not shown). To

analyze whether production of ROS depends on TNF-α, monocytes were treated with both TNF-α Ab and IL-19, and ROS production was monitored. As shown in Fig. 9*C*, when monocytes were treated with TNF-α for 30 min followed by IL-19 stimulation for another 30 min (Fig. 9*C*, column C and curve C), ROS production was partially inhibited. However, if monocytes were treated with IL-19 for 30 min followed by incubation with TNF-α Ab, ROS production was not inhibited (Fig. 9*C*, column D and curve D). If both IL-19 and TNF-α were added at the same time (Fig. 9*C*, column E and curve E), the extent of inhibition on ROS production was not as great as when TNF-α Ab was added first. These results indicate that ROS production may not be completely dependent on TNF-α production.

Discussion

The present study demonstrates that human IL-19 genes consist of seven exons and six introns and that the coding region was encoded by exons 3–7. There are two exons in the 5′-untranslated region. Several transcription variants in the 5′-untranslated region generated by alternative splicing were found during isolation of a full-length clone by 5′ RACE. This observation was similar to results previously described (16). Gallagher et al. (16) showed that human IL-19 consists of five exons and four introns in the coding region. They also found another longer form transcript containing an alternative translation start site which is in-frame with the rest of the IL-19 mRNA, so they predicted that there is one intron near the methionyl residue. These variants were translated into identical mature proteins. Whether or not the variation of the 5′-untranslated region has any effect on the efficiency of the translation awaits further study.

The analysis of the human IL-19 promoter region showed a fragment of 394 bp (pA), including 247 bp of exon 1 that supports luciferase activity at a level 7- to 8-fold greater than that of the negative control. The fluctuation of promoter activity in pA, pB, pC, pD, and pE may be due to some repressor or enhancer sequences located in these regions, such as the sequences between −1858 and −147. We will perform an EMSA to determine the positive or negative sequence on the promoter region and potential transcription factors in the cell lysate involved in the regulation.

The promoter region of IL-10 has been shown to be involved in many mechanisms of IL-10 activities. For example, AP-1 and SP-1 were shown to play an important role in regulating IL-10 function (19). Several diseases have been shown to be associated with polymorphism of the IL-10 promoter region. It was shown that high IL-10 production associated with autoimmune disease, including rheumatoid arthritis and systemic lupus erythematosus, may be a genetic risk factor for disease susceptibility (20). The basis for a heritable difference in IL-10 production is not well known. The IL-10 gene promoter is polymorphic, and promoter-reporter studies have identified several positive and negative regulatory sequences within the 1.3-kb region upstream of the transcription start site. Several single-nucleotide polymorphisms (SNP) have also been identified in this region. All these results demonstrate that IL-10 promoter sequences may be a central mediator of its function. Searching the human genome SNP database, we found four potential SNPs on the 2105 bp of the pA fragment in the human IL-19 promoter region. Whether these four potential SNPs of human IL-19 are also associated with any inflammatory diseases awaits further study.

Analysis of the MDA-7 (IL-24) gene, another member of the IL-10 family, has demonstrated that AP-1 and C/EBP transcription factor contributed to its promoter activity during human melanoma differentiation (21). This finding provided insights into the regulation mechanism of the MDA-7 gene during induction of terminal cell differentiation in human melanoma cells. The IL-19 promoter region also contains AP-1- and C/EBP-binding sites. Whether or not IL-19 and MDA-7 share some similar mechanism in gene regulation by the regulatory element of AP-1 and C/EBP awaits detailed study of these sequences.

In the promoter region of IL-19, there are several copies of keratinocytes enhancer element (AARCAAA). Another member of IL-10 family, IL-20, has been shown to be involved in the proliferation of keratinocytes (10). It will be interesting to study whether IL-19 also has any association with keratinocytes function by the keratinocyte enhancer element in its promoter region.

In addition to expression of IL-19 in *E. coli*, we expressed IL-19 in the yeast *P. pastoris* system. Protein purified from the culture medium of the yeast showed three different sizes of the molecule with identical amino acids analyzed by mass spectrophotometry. The heterogeneity of the protein may be due to different levels of glycosylation, which is similar to what was observed in the mammalian expression system (16).

We also observed dimerization of recombinant IL-19 protein when the pure protein was run on a nonreduced gel. This indicated that, as with IL-10, a homodimer of IL-19 may be the functional unit.

IL-10 suppresses the release and function of a number of proinflammatory cytokines, such as IL-1, IL-6, and TNF-α (2, 3). We found, however, that both human and mouse IL-19, a homologue of IL-10, stimulated monocytes to produce IL-6 and TNF-α. Therefore, IL-19 may play an immune response role different from that of IL-10. The data shown in Fig. 7 also demonstrated that IL-10 completely inhibited the induction of IL-6 and TNF-α by IL-19 if monocytes were pretreated with IL-10 followed by IL-19. However, if IL-10 was added to monocytes 2 h after IL-19, it only partially inhibited IL-6 production (~12% activity). In contrast, TNF-α induction can be completely inhibited because level of TNF-α is same as that of IL-10 treated alone. These results indicated that induction of IL-6 and TNF-α may occur at different stages of incubation with IL-19. Alternatively, regulation of IL-6 production by IL-19 and IL-10 may take different mechanisms in signal transduction.

Moreover, IL-6 attenuates the synthesis of the proinflammatory cytokines while having little effect on the synthesis of anti-inflammatory cytokines, such as IL-10 and TGF-β. IL-6 promotes the synthesis of IL-1 receptor antagonist and soluble TNF-αR release in humans (22). We may then speculate that IL-19 plays an important role in inflammation.

The result illustrated by Fig. 9*C* demonstrated that IL-19 induced ROS production which could be only partially inhibited by TNF-α Ab. It indicated that ROS production induced by IL-19 may not completely depend on TNF-α. Moreover, when monocytes were preincubated with IL-19 for 30 min followed by the addition of TNF-α Ab, production of ROS was not only not inhibited but also enhanced. The reason for this was not clear. We also found that a high level of ROS production could be induced rapidly during the first 30 min when a higher concentration of IL-19 (200 ng/ml) was used to stimulate monocytes (data not shown). Therefore, we may speculate that ROS production induced by high concentration of IL-19 is not mediated through TNF-α, because 30 min was not long enough for TNF-α protein to be synthesized.

IL-10 has been shown to inhibit generation of ROS in macrophages (23). Treatment of macrophages with LPS caused activation of NF-κB and rapid proteolysis of IκB-α degradation in the cells. IL-10 pretreatment inhibited both NF-κB activation and IκB-α degradation. Both processes were also inhibited by ROS

scavengers, demonstrating that inhibition of IL-10 on NF-κB activation and IκB-α degradation was mediated through ROS production. When IL-10-deficient mice were used to test whether IL-10, through ROS, protects endothelial cells from inflammation, it was shown that IL-10 protects endothelial function after an acute inflammatory stimulus by limiting local increases in superoxide (24). Our results demonstrated that IL-19 induced production of ROS in monocytes, contrary to what was observed with IL-10. Taken together, IL-19, sharing some homology with IL-10, demonstrated biologic functions quite distinct from those of IL-10.

In summary, we have isolated the full-length human IL-19 cDNA and identified its genomic clone. The human IL-19 gene consists of seven exons and six introns and is encoded by exons 3–7. Several different transcripts were generated by alternative splicing at their 5′-untranslated region. These transcript variants seemed to encode the same amino acid sequences as the mature protein (16). A fragment containing 394 bp upstream of exon 1 showed promoter activity 7- to 8-fold greater than that of the negative control. A fragment (from −1858 bp to −147 bp) further upstream of 1712 bp may contain repressor or enhancer sequences, because the presence of these sequences affected the promoter activity of 394 bp.

IL-19 can induce IL-6 and TNF-α production in monocytes and result in cell apoptosis. Because our assay system was an in vitro analysis, cell apoptosis was observed in a pure population of monocytes (95% pure). The observation of apoptosis on the monocytes themselves may not reflect the true activity in vivo. It is possible that monocytes may use the production of TNF-α to cause apoptosis in other cells as a defense mechanism against infection or in tumor cell eradication after receiving a signal from IL-19. In other words, it may be a paracrine and not an autocrine effect. Our results also demonstrated that IL-19 induced monocytes to produce ROS. Whether or not ROS production plays an important role as a mediator of the functions of IL-19 awaits further comprehensive study. In contrast to IL-19, IL-10 inhibits production of TNF-α, IL-6, cell apoptosis, and ROS production. These results demonstrate that the activities and functions of IL-19 and IL-10 are different. IL-10 was used as an anti-inflammatory drug in clinical trials. We therefore speculate that the antagonist of IL-19 may be the molecule to be applied in clinics, if IL-19 can be demonstrated to be associated with any immune disorder diseases.

Acknowledgments

We thank Dr. Chiang-Ting Chien from National Taiwan University for instruction on ROS production analysis.

References

1. O'Farrell, A. M., Y. Liu, K. W. Moore, and A. L. Mui. 1998. IL-10 inhibits macrophage activation and proliferation by distinct signaling mechanisms: evidence for Stat3-dependent and -independent pathways. *EMBO J. 17:1006.*
2. Gesser, B., H. Leffers, T. Jinquan, C. Vestergaard, N. Kirstein, S. Sindet-Pedersen, S. L. Jensen, K. Thestrup-Pedersen, and C. G. Larsen. 1997. Identification of functional domains on human interleukin 10. *Proc. Natl. Acad. Sci. USA 94:14620.*
3. Ding, Y., L. Qin, S. V. Kotenko, S. Pestka, and J. S. Bromberg. 2000. A single amino acid determines the immunostimulatory activity of interleukin 10. *J. Exp. Med. 191:213.*
4. Go, N. F., B. E. Castle, R. Barrett, R. Kastelein, W. Dang, T. R. Mosmann, K. W. Moore, and M. Howard. 1990. Interleukin 10, a novel B cell stimulatory factor: unresponsiveness of X chromosome-linked immunodeficiency B cells. *J. Exp. Med. 172:1625.*
5. Thompson-Snipes, L., V. Dhar, M. W. Bond, T. R. Mosmann, K. W. Moore, and D. M. Rennick. 1991. Interleukin 10: a novel stimulatory factor for mast cells and their progenitors. *J. Exp. Med. 173:507.*
6. Rousset, F., E. Garcia, T. Defrance, C. Peronne, N. Vezzio, D. H. Hsu, R. Kastelein, K. W. Moore, and J. Banchereau. 1992. Interleukin 10 is a potent growth and differentiation factor for activated human B lymphocytes. *Proc. Natl. Acad. Sci. USA 89:1890.*
7. de Waal, M. R. 1998. Interleukin-10. In *Cytokine.* A. R. Mire-Sluis, and R. Thorpe, eds. Academic Press, San Diego, p. 151.
8. de Waal, M. R., J. Abrams, B. Bennett, C. G. Figdor, and J. E. de Vries. 1991. Interleukin 10 (IL-10) inhibits cytokine synthesis by human monocytes: an autoregulatory role of IL-10 produced by monocytes. *J. Exp. Med. 174:1209.*
9. Dumoutier, L., C. Leemans, D. Lejeune, S. V. Kotenko, and J. C. Renauld. 2001. Cutting edge: STAT activation by IL-19, IL-20 and mda-7 through IL-20 receptor complexes of two types. *J. Immunol. 167:3545.*
10. Blumberg, H., D. Conklin, W. F. Xu, A. Grossmann, T. Brender, S. Carollo, M. Eagan, D. Foster, B. A. Haldeman, A. Hammond, et al. 2001. Interleukin 20: discovery, receptor identification, and role in epidermal function. *Cell 104:9.*
11. Dumoutier, L., J. Louahed, and J. C. Renauld. 2000. Cloning and characterization of IL-10-related T cell-derived inducible factor (IL-TIF), a novel cytokine structurally related to IL-10 and inducible by IL-9. *J. Immunol. 164:1814.*
12. Dumoutier, L., E. Van Roost, D. Colau, and J. C. Renauld. 2000. Human interleukin-10-related T cell-derived inducible factor: molecular cloning and functional characterization as an hepatocyte-stimulating factor. *Proc. Natl. Acad. Sci. USA 97:10144.*
13. Rich, B. E., and T. S. Kupper. 2001. Cytokines: IL-20: a new effector in skin inflammation. *Curr. Biol. 11:R531.*
14. Jiang, H., J. J. Lin, Z. Z. Su, N. I. Goldstein, and P. B. Fisher. 1995. Subtraction hybridization identifies a novel melanoma differentiation associated gene, mda-7, modulated during human melanoma differentiation, growth and progression. *Oncogene 11:2477.*
15. Knappe, A., S. Hor, S. Wittmann, and H. Fickenscher. 2000. Induction of a novel cellular homolog of interleukin-10, AK155, by transformation of T lymphocytes with *Herpesvirus saimiri. J. Virol. 74:3881.*
16. Gallagher, G., H. Dickensheets, J. Eskdale, L. S. Izotova, O. V. Mirochnitchenko, J. D. Peat, N. Vazquez, S. Pestka, R. P. Donnelly, and S. V. Kotenko. 2000. Cloning, expression and initial characterization of interleukin-19 (IL-19), a novel homologue of human interleukin-10 (IL-10). *Genes Immun. 1:442.*
17. Oren, M., and C. Prives. 1996. p53: upstream, downstream and off stream. Review of the eighth p53 workshop (Dundee, July 5–9, 1996). *Biochim. Biophys. Acta 1288:R13.*
18. Darzynkiewicz, Z., S. Bruno, G. Del Bino, W. Gorczyca, M. A. Hotz, P. Lassota, and F. Traganos. 1992. Features of apoptotic cells measured by flow cytometry. *Cytometry 13:795.*
19. Brightbill, H. D., S. E. Plevy, R. L. Modlin, and S. T. Smale. 2000. A prominent role for Sp-1 during lipopolysaccharide-mediated induction of the IL-10 promoter in macrophages. *J. Immunol. 164:1940.*
20. Gibson, A.W., J. C. Edberg, J. Wu, R. G. Westendorp, T. W. Huizinga, and R. P. Kimberly. 2001. Novel single nucleotide polymorphisms in the distal IL-10 promoter affect IL-10 production and enhance the risk of systemic lupus erythematosus. *J. Immunol. 166:3915.*
21. Madireddi, M. T., P. Dent, and P. B. Fisher. 2000. AP-1 and C/EBP transcription factors contribute to mda-7 gene promoter activity during human melanoma differentiation. *J. Cell. Physiol. 185:36.*
22. Opal, S. M., and V. A. DePalo. 2000. Anti-inflammatory cytokines. *Chest 117: 1162.*
23. Dokka, S., X. Shi, S. Leonard, L. Wang, V. Castranova, and Y. Rojanasakul. 2001. Interleukin-10-mediated inhibition of free radical generation in macrophages. *Am. J. Physiol. Lung Cell Mol. Physiol. 280:L1196.*
24. Gunnett, C. A., D. D. Heistad, D. J. Berg, and F. M. Faraci. 2000. IL-10 deficiency increases superoxide and endothelial dysfunction during inflammation. *Am. J. Physiol. Heart Circ. Physiol. 279:H1555.*